Mon. Not. R. Astron. Soc. **000**, 000–000 (0000) Printed 4 January 2012 (MN LaTeX style file v2.2)

Discovery of the black hole mass and soft lag relation in active galactic nuclei

B. De Marco,[1,2⋆] G. Ponti,[3] M. Cappi,[2] M. Dadina,[2] P. Uttley,[4], E. M. Cackett[5,6], A. C. Fabian,[6] and G. Miniutti[7]

[1]*Dipartimento di Astronomia, Università di Bologna, via Ranzani 1, I-40127 Bologna, Italy*
[2]*Istituto di Astrosica Spaziale e Fisica Cosmica-Bologna, INAF, via Gobetti 101, I-40129 Bologna, Italy*
[3]*Faculty of Physical and Applied Science, University of Southampton, Southampton SO17 1BJ, UK*
[4]*Astronomical Institute "Anton Pannekoek", University of Amsterdam, Postbus 94249, 1090 GE Amsterdam, The Netherlands*
[5]*Wayne State University, Department of Physics and Astronomy, Detroit, MI, 48201, USA*
[6]*Institute of Astronomy, Madingley Road, Cambridge CB3 0HA, UK*
[7]*Centro de Astrobíologia (CSIC-INTA), Dep. de Astrofísica; LAEFF, PO Box 78, E-28691, Villanueva de la Cañada, Madrid, Spain*

Released 2011 Xxxxx XX

ABSTRACT

We carried out a systematic analysis of time lags between X-ray energy bands in a large sample (32 sources) of unabsorbed, radio quiet active galactic nuclei (AGN), observed by XMM-Newton. The analysis of X-ray lags is performed in the Fourier-frequency domain, between energy bands where the soft excess (soft band) and the primary power law (hard band) dominate the emission. We detected a soft/negative lag in a total of 15 out of 32 sources. Considering that 7 of these have not been previously reported in the literature, this work more than doubles the number of known sources with a soft/negative lag. The characteristic time-scales (i.e. frequency and amplitude) of the soft/negative lag do show a highly significant (i.e. $\gtrsim 4\sigma$) correlation with the black hole mass. The measured correlations indicate that soft lags are systematically shifted to lower frequencies and higher absolute amplitudes as the mass of the source increases. To first approximation, all the sources in the sample are consistent with having similar mass-scaled lag properties. These results clearly demonstrate the existence of a mass-scaling law for the soft/negative lag, that holds for AGN spanning a large range of masses (about 2.5 orders of magnitude), thus supporting the idea that soft lags originate in the innermost regions of AGN and are powerful tools for testing their physics and geometry.

Key words: galaxies: active, galaxies: nuclei, X-rays: galaxies

1 INTRODUCTION

The observed similarities in the timing properties of different black hole (BH) systems suggest that the same physical mechanism is at work in sources spanning a wide range of masses (e.g. Uttley et al 2005, McHardy et al 2006). This observational fact represents an important achievement in the context of the theory of unification of BH accretion. A breakthrough in this respect was the discovery of the mass-scaling law that regulates the characteristic time-scales of variability, identified with the high frequency break in the power spectral density function (PSD). This relation holds for objects of widely different size (i.e. over about eight order of magnitudes in mass, from BH X-ray binaries, BHXB, up to active galactic nuclei, AGN, McHardy et al 2006, Koerding et al 2007) and is in agreement with expectations from standard accretion disk models, whereby all the characteristic time-scales depend linearly on the BH mass, $M_{\rm BH}$ (e.g. Treves et al 1988).

Another fundamental analogy emerges from the comparison of time lags between X-ray energy bands. Hard/positive lags (i.e. hard X-ray band variations lagging soft X-ray band variations) are generally observed in both BHXBs and AGN, and can be interpreted as propagation of mass accretion rate fluctuations in the disc (Kotov et al. 2001 and Arévalo & Uttley 2006a). Those lags are usually detected at relatively low fequencies (i.e. below the PSD high frequency break).

On the other hand, a relatively new and interesting perspective comes from the study of high frequency, soft/negative lags (i.e. soft X-ray band variations lagging hard X-ray band variations). The first significant detection of a soft/negative lag was reported in the narrow line Seyfert 1 (NLSy1) galaxy 1H0707-495 (Fabian et al 2009, Zoghbi et al 2010), and interpreted as the signature of relativistic reflection which "reverberates" in response to continuum changes after a time equal to the light-crossing time from the source to the reflecting region. A different interpretation has been proposed in terms of a complex system of scatterers/absorbers located close to the line of sight, but at hundreds of gravitational radii, r_g, from the

⋆ E-mail: demarco@iasfbo.inaf.it

central source (Miller et al 2010), thus requiring us to have a special line of sight to the source.
Subsequently, soft lags have been observed in several other sources (e.g. Tripathi 2011, Emmanoulopoulos et al 2011, Zoghbi & Fabian 2011). One of the largest mass sources ($M_{\rm BH} \sim 10^{7-8} M_{\odot}$) showing a soft/negative lag is PG 1211+143 (De Marco et al 2011), whose lag spectrum appears "shifted" by about one order of magnitude (being the lag frequency, ν, and amplitude, τ, found at $\sim 1-6\times10^{-4}$Hz and $\sim 10^2$ s, respectively) with respect to those measured in other low mass sources (i.e. $\nu \sim 10^{-3}$Hz and $\tau \sim 20-30$ s, Emmanoulopoulos et al 2011). In De Marco et al (2011) we speculated that this difference could be simply explained if the time-scales in PG 1211+143 are scaled-up by the BH mass, estimated to be about 10-100 times the mass of the other AGN for which X-ray lags have been recorded so far. In this Letter we explore this hypothesis, by studying the properties of the lag frequency spectrum in a large sample of sources, spanning a wide range of masses (about 2.5 decades). The time-scales of detected soft/negative lags are then used to study correlations with relevant parameters, such as luminosity and BH mass.

2 THE SAMPLE

The sources analysed are extracted from the *CAIXAvar* sample – a subsample of the CAIXA sample by Bianchi et al (2009a) – presented in Ponti et al. (2011), which includes all the well-exposed, X-ray unobscured ($N_H < 2\times10^{22}$cm^{-2}), radio quiet AGN observed by *XMM-Newton* in targeted observations as of June 2010. We considered all the sources having at least one observation with a longer than 40 ks exposure (41 sources), and selected those with published black hole mass, $M_{\rm BH}$, estimates (39 sources). Finally, we excluded all sources for which Ponti et al (2011) estimated an excess variance consistent with zero, i.e. those consistent with having constant flux during the observations analysed here, on the time-scales of interest for this work ($\lesssim$ 40ks). With the latter selection our final sample reduced to a total of 32 sources. For each source all the available observations in the XMM-Newton archive have been used in our analysis, apart from those highly corrupted by background flares. In the computation of the lag-frequency spectra, multiple observations have been combined to obtain better statistics.
Only data from the EPIC-pn camera were used, because of its high effective area and S/N over the 0.3-10 keV energy band. Data reduction was performed using XMM Science Analysis System (SAS v. 10.0), starting from the Observation Data Files (ODF) and following standard procedures. Filtered events are characterized by PATTERN $\leqslant$4, and are free from background flares. Typical source extraction regions are 45 arcsec radius circles. Spectra were extracted and used to select the energy bands for the computation of time lags. They were grouped to a minimum of 20 counts per bin, while response matrices were generated through the RMFGEN and ARFGEN SAS tasks.

3 LAG VS FREQUENCY SPECTRA

We computed lag-frequency spectra between light curves in the soft and hard X-ray energy bands following the techniques described in detail by Nowak et al (1999) and applied to XMM-Newton data in De Marco et al (2011). The energy bands vary slightly from source to source, to account for changes in spectral complexities. In general, they were selected so as to single out energies dominated by the soft excess and the primary power law, and are roughly defined in the intervals 0.3-1 keV (soft) and 1-5 keV (hard). Data above this energy were excluded so as to ensure a high S/N ratio. Sources for which a negative lag was reported in the literature have been re-analyzed with our procedures. We set as the detection threshold the 2σ significance level. Since coherence must be non zero for the lag to be reliable, we checked whether the coherence level was high enough in the frequency range where each negative lag is detected, and marked as spurious all those characterized by coherence consistent with zero. The soft/negative lags reported in this Letter are all characterized by a medium-to-high level of intrinsic coherence ($0.4 \lesssim \gamma^2 \lesssim 1$) at the frequencies of interest, this value representing the fraction of the signal that is responsible for the lag.
Fig. 4 displays the lag-frequency spectra of sources showing a negative lag (see also Table 1 for details about the sources). We detect a soft/negative lag in 15 out of 32 sources. The negative lags of well known objects (Ark 564, 1H0707-495, Mrk 1040, Mrk 766, MCG-6-30-15, RE J1034+396, NGC 3516, PG 1211+143) are perfectly consistent with previously published results (Arévalo et al 2006b, Zoghbi et al 2010, Tripathi et al 2011, Emmanoulopoulos et al 2011, Zoghbi & Fabian 2011, Turner et al 2011, De Marco et al 2011), despite the fact that sometimes the adopted energy bands are slightly different from those in original papers. Moreover, we report a total of 7 newly detected soft lags (i.e. NGC 4395, NGC 4051, NGC 7469, Mrk 335, NGC 6860, NGC 5548, Mrk 841). The observed values of lag amplitudes and frequencies span about two decades (i.e. $\tau \sim 10-600$ s and $\nu \sim 0.07-4\times10^{-3}$ Hz), similar to the sampled BH mass range of values ($\sim 0.1-10\times10^{7} M_{\odot}$).

4 LAG CORRELATIONS

The measured lag-frequency spectra are characterized by similar profiles, with the negative lag shifting to lower frequencies as the mass of the source increases (see Fig. 4, where the plots are in order of increasing mass of the source). It is thus interesting to test the hypothesis of a $M_{\rm BH}$ dependence of the lag characteristic time-scales (i.e. amplitude and frequency).
The sources showing a soft/negative lag are characterized by widely different mass values, spanning about 2.5 orders of magnitude in estimated $M_{\rm BH}$. The $M_{\rm BH}$ values adopted in this Letter are taken from the literature (see Table 1 for references) and are preferably those obtained from reverberation mapping and stellar velocity dispersion techniques. In all the other cases (5 out of 15) we considered estimates obtained from the empirical relation between the optical luminosity at 5100Å and the broad line region size (R_{BLR}, e.g. Bentz et al 2009). The unknown mass uncertainties have been replaced with the estimated dispersion of the adopted relation for mass determination (i.e. 0.5 dex in the case of single epoch methods, and 0.4 dex for the others).
Fig. 1 shows the lag frequency and amplitude vs mass ($\nu_{\rm lag}$ vs $M_{\rm BH}$ and τ vs $M_{\rm BH}$) on a logarithmic scale. In the plots the $\nu_{\rm lag}$ and τ quantities correspond to the frequency and amplitude of the minimum negative lag detected for each source, once corrected for the redshift of the source. To statistically assess whether the pairs of parameters are correlated we computed the Spearman's rank correlation coefficient, ρ. The test yielded $\rho \sim -0.78$ and $\rho \sim 0.90$ respectively for the $\nu_{\rm lag}$ and τ parameters, both corresponding to a correlation with significance of $\gtrsim 4\sigma$. We tested whether the correlation could be an artifact of the variability power of the sources decreasing with increasing mass, which may induce a shift (towards lower values) of the frequency at which the Poisson noise compo-

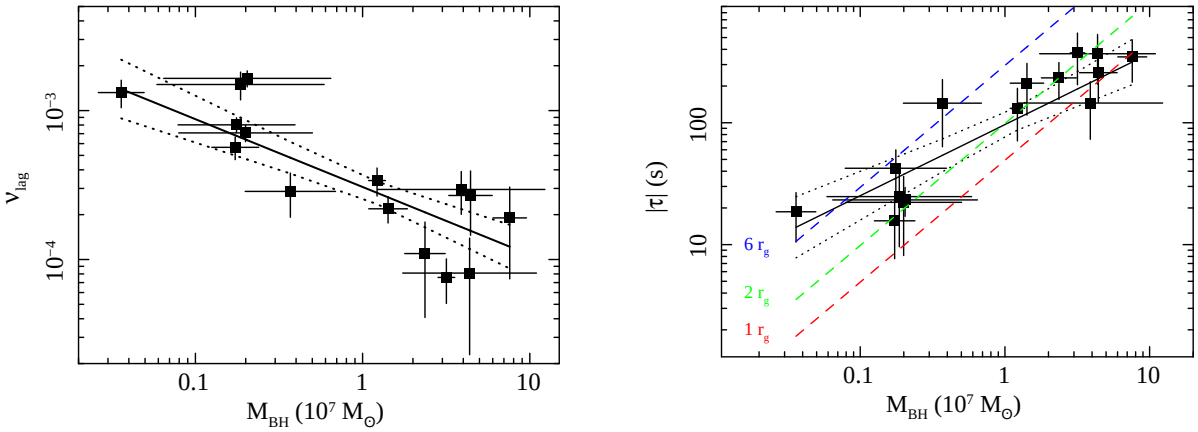

Figure 1. Negative lag frequency ($\nu_{\rm lag}$) vs $M_{\rm BH}$ (*left panel*) and absolute amplitude (| τ |) vs $M_{\rm BH}$ (*right panel*) trends (error bars represent the 1-σ confidence interval, the frequency and amplitude of lag are corrected for the redshift). The best fit linear models and the combined 1-σ error on the slope and normalization are overplotted as continuous and dotted lines. The dashed lines in the right panel represent the light crossing time at $1r_{\rm g}$, $2r_{\rm g}$, and $6r_{\rm g}$ as a function of mass.

nent dominates, quenching the soft lag. Using results from all the sources of the sample, we correlated the frequency where the observed coherence drops below 0.2 (being the high frequency drop in coherence caused by Poisson noise) with BH mass. This test yields $\rho \sim -0.41$, which corresponds to a low significance (~89 per cent) for the correlation with the BH mass, suggesting that the relation is not driven by this effect.

It is worth noting that the lag profile in the large mass sources is not well-sampled, since the data are limited (at lower frequencies) by the duration of the observations. Hence, we checked whether the correlation still holds when considering these points as upper/lower limits for the lag frequency/absolute amplitude, by computing generalised Kendall's rank correlation statistics for censored data sets (e.g. Isobe et al 1986). Although slightly lower, the significance of the correlation is still relatively high ($> 3\sigma$).

Following Bianchi et al (2009b), we applied a least squares linear regression approach to derive constraints on the functional dependence of $\nu_{\rm lag}$ and τ from $M_{\rm BH}$. To minimize the uncertainty in the best fit model we carried out 1000 MonteCarlo simulations, whereby the x- and y-axis coordinates of each experimental point were substituted by two random values drawn from two Gaussian distributions with means equal to the coordinates of the data point on each axis and the associated statistical uncertainty as standard deviation (see Bianchi et al 2009b). Each simulated data set was fitted in log-log space with a linear model. The mean of the slopes and intercepts were used to define our best fit model, while the mean standard deviation represents the uncertainty of the best fit parameters. The results of the fits are Log $\nu_{\rm lag}$ = $-3.51[\pm0.07] - 0.46[\pm0.09]$ Log(M_7) and Log | τ |= $1.98[\pm0.09]+0.58[\pm0.11]$ Log(M_7), where $M_7 = M_{\rm BH}/10^7 M_\odot$. The estimated scatter around the best fit model is $\sigma_s \sim 0.22$ and 0.24, respectively for the τ–$M_{\rm BH}$ and $\nu_{\rm lag}$–$M_{\rm BH}$ relations. It is worth noting that the small scatter in the relation is consistent with being mostly due to the uncertainty in BH mass determination, being of the same order of the intrinsic scatter in reverberation mass estimates. The best fit and the 1-σ combined uncertainty on the model parameters have been overplotted on the data in Fig. 1. We notice that, although statistically not consistent with a linear relation, the best fit slopes increase and become consistent with linear scaling, if the data from the larger mass objects are treated as upper/lower limits for the lag frequency/absolute amplitude. Finally, we checked

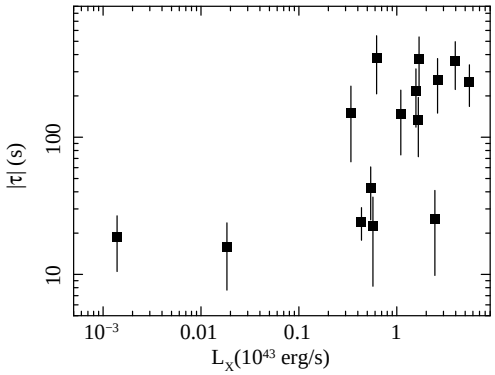

Figure 2. Negative lags absolute amplitude (| τ |) vs 2-10 keV luminosity (errors bars represent the 1-σ confidence interval).

whether the lag time-scales exhibit some dependence on the source X-ray luminosity between $E = 2 - 10$ keV (see Fig. 2), but a less significant correlation was found ($< 3\sigma$ and $< 2\sigma$ respectively for τ and $\nu_{\rm lag}$), which further decreases ($< 2\sigma$) when looking at the correlation with the bolometric luminosity (as computed using the correction factor by Marconi et al 2004). These results support the hypothesis that the main parameter driving the correlation is the BH mass.

Non-detections: we checked whether the absence of a soft/negative lag in the remaining 17 sources may be real or due to poor statistics. Hence, for each lag-frequency spectrum we recorded the minimum lag value amplitude and its frequency in the interval where the coherence is not consistent with zero. We collected a total of 10 marginal soft lags with significance between 1-2σ and 7 with significance $< 1\sigma$ (examples are shown in Fig. 5). Results are shown in Fig. 3 (where, for brevity, only the $\tau-M_{\rm BH}$ data points are shown, overplotted on the 15 soft lag detections at $> 2\sigma$ confidence level) where the $> 1\sigma$ detections are displayed with error bars, while the $< 1\sigma$ are marked as 90 per cent upper limits. The agreement with the overall correlation is clear, with the significance increasing to $> 5\sigma$ confidence level ($\rho \sim 0.73$ and 0.86, respectively for the frequency and amplitude vs BH mass correlations). We conclude that none of the remaining 17 sources is, with the available data, significantly outside the observed correlation and that all the sources are

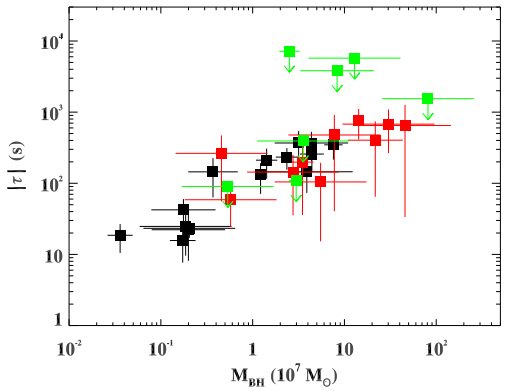

Figure 3. The 10 marginal soft lags with significance between 1-2σ (red data points) and the 7 with significance $< 1\sigma$ (green upper limits) overplotted to the 15 detections at $> 2\sigma$ (black data points).

consistent with showing the same lag properties. The low detection significance of the soft lag in these sources is mainly due to poor statistics issues (e.g. limited exposure, small number of observations, low variability power, etc.), which are most relevant in large mass sources, where the expected lag frequency is of the order of the minimum sampled frequency.

5 DISCUSSION

The systematic analysis of X-ray lags we carried out in the Letter doubled the number of soft lags so far detected in AGN (15 out of 32 sources) and led us to the discovery of a highly significant ($\gtrsim 4\sigma$) correlation between the time-scales (frequency and amplitude) of the detected soft/negative lag and the black hole mass. Moreover, data from the remaining 17 sources are consistent with the observed correlation, the significant detection of a soft lag being precluded only by poor statistics in these observations. Hence, we conclude that a soft lag, scaling with the mass of the BH, cannot be excluded in any of the 32 sources of our sample. This result confirms our previous inference (De Marco et al 2011), whereby the negative lag detected in PG 1211+143 was suggested to represent the large mass counterpart of negative lags detected in lower mass sources (such as 1H0707-495). Most importantly it highlights a fundamental property of soft lags, namely the fact that they depend on the BH mass. For example, in a reverberation scenario, this is naturally expected, given that the gravitational radius light crossing time ($t_c = r_g/c$, where $r_g = GM/c^2$ is the gravitational radius) scales linearly with the mass of the central object. Despite the inferred best fit slopes for the observed lag-$M_{\rm BH}$ trends are statistically different from a linear relation, we notice that the data are biased against an intrinsically steeper dependence. Indeed the large mass sources are sensitive to the length of the observation, which does not allow to measure the lag profile over frequencies lower than the inverse of the observation length. Albeit not introducing any spurious correlation, the effect of these biases is to induce a flattening of the intrinsic one. Indeed, when the large BH mass data points are treated as upper/lower limits the slope of the correlations becomes steeper. A sample including longer and more sensitive observations would be necessary to accurately determine the real slope of the relation.

A thorough study of the implications of the lag-$M_{\rm BH}$ correlation, as inferred from our analysis, on the proposed soft lags models is beyond the aim of this Letter. However, it is worth noting that a BH mass dependence of the characteristic time-scales is naturally expected in standard accretion disc models. In Fig. 1 we overplotted as a reference the light crossing time at $1r_{\rm g}$, $2r_{\rm g}$, and $6r_{\rm g}$ as a function of BH mass. The observed soft lags roughly lay in this range of time-scales, meaning that the involved distances are quite small and, again, mass-dependent. Moreover, the evidence for a soft lag being present in such a large number of sources is at odds with expectations from models that need the single objects to be on a special line of sight for the measured lag to be observable. Overall these results are consistent with a scenario whereby the delayed soft excess emission originates in the innermost regions of the accretion disc, and is triggered by a compact central source of hard X-rays. Hence, a thorough understanding of soft lags properties will allow to probe the physics and geometry of the innermost regions of AGN.

ACKNOWLEDGMENTS

This work is based on observations obtained with XMM-*Newton*, an ESA science mission with instruments and contributions directly funded by ESA Member States and NASA. GP acknowledges support via an EU Marie Curie Intra-European Fellowship under contract no. FP7-PEOPLE-2009-IEF-254279. BDM, MC, and MD thank financial support from the ASI/INAF contract I/009/10/0.

REFERENCES

Arévalo P., Uttley P., 2006a, MNRAS, 367, 801
Arévalo P., Papadakis I. E., Uttley P., McHardy I. M., Brinkmann W., 2006b, MNRAS, 372, 401
Bentz M. C., 2009, ApJ, 705, 217
Bianchi S., Guainazzi M., Matt G., Fonseca Bonilla N., Ponti, G., 2009a, A&A, 495, 421
Bianchi S., Bonilla N. F., Guainazzi M., Matt G., Ponti G., 2009b, A&A, 501, 915
De Marco B., Ponti G., Uttley P., Cappi M., Dadina M., Fabian A. C., Miniutti G., 2011, MNRAS, 417, 98
Emmanoulopoulos D., McHardy I. M., Papadakis I. E., 2011, MNRAS, 416, 94
Fabian A. C., et al., 2009, Nat, 459, 540
Isobe T., Feigelson E. D., Nelson P. I., 1986, ApJ, 306, 490
Koerding E. G., et al., 2007, MNRAS, 380, 301
Kotov O., Churazov E., Gilfanov M., 2001, MNRAS, 327, 799
Marconi A., Risaliti G., Gilli R., Hunt L. K., Maiolino R., & Salvati, M. 2004, MNRAS, 351, 169
McHardy I. M., Koerding E., Knigge C., Uttley P., Fender R. P., 2006, Nat, 444, 730
Miller L., Turner T. J., Reeves J. N., Braito V., 2010, MNRAS, 408, 1928
Nowak M. A., Wilms J., Dove J. B., 1999, ApJ, 517, 355
Ponti G., et al, 2011, arXiv:1112.2744
Treves A., Maraschi L., Abramowitz M., 1988, PASP, 100, 427
Tripathi S., Misra R., Dewangan G., Rastogi S., 2011, ApJ, 736, 37
Turner T. J., Miller L., Kraemer S. B., Reeves J. N., 2011, ApJ, 733, 48
Uttley P., McHardy I. M., Vaughan S., 2005, MNRAS, 359, 345
Zoghbi A., et al, 2010, MNRAS, 401, 2419
Zoghbi, A., Fabian, A. C., 2011, MNRAS, tmp 1844Z

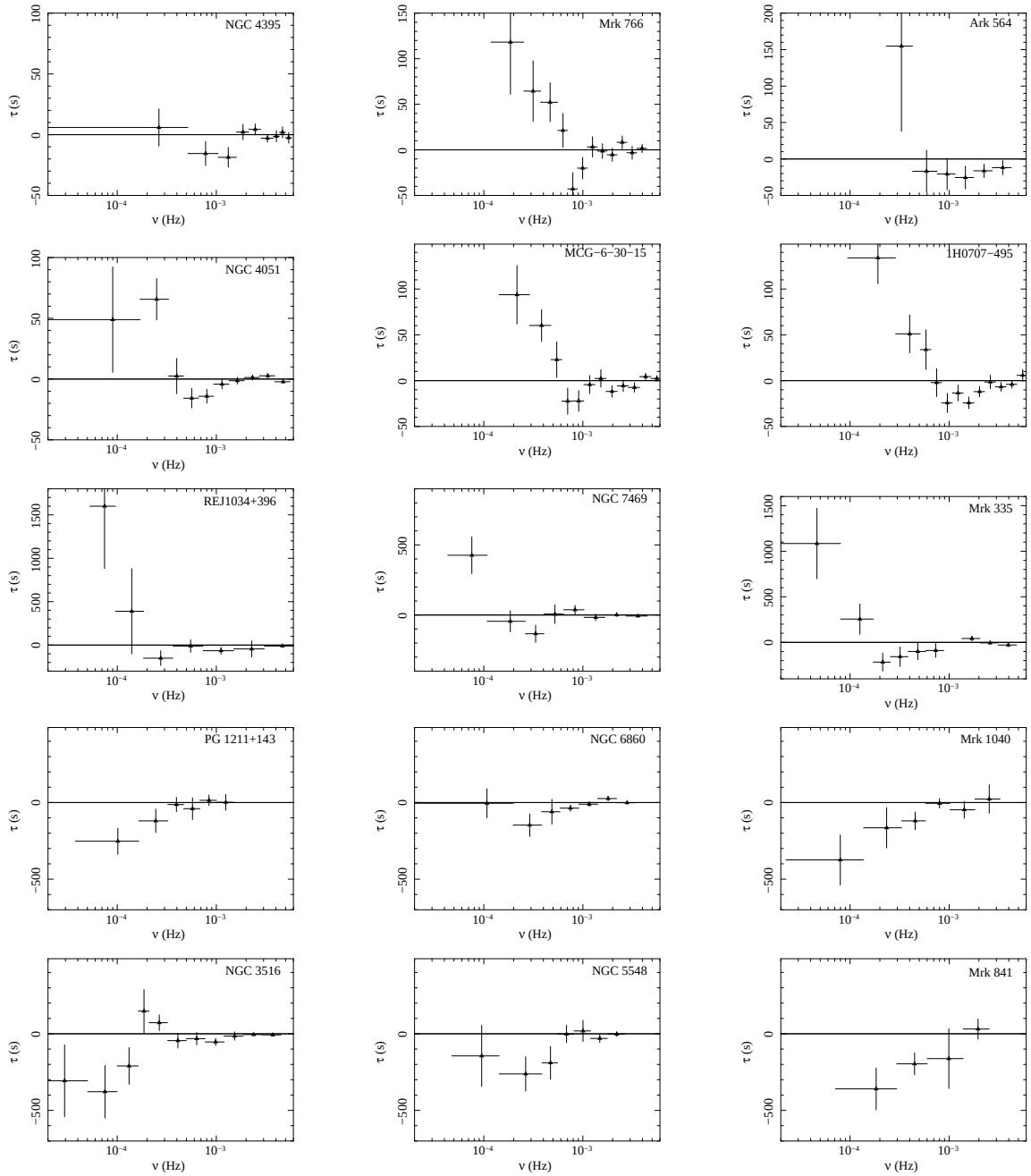

Figure 4. Lag-frequency spectra of sources with a detected soft/negative lag at $> 2\sigma$ confidence level, in order of increasing mass (from top left to bottom right).

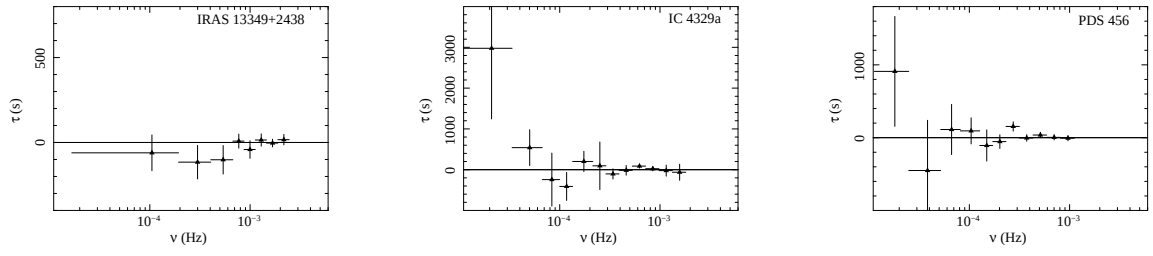

Figure 5. Examples of lag-frequency spectra of sources with a marginal negative lag at 1.8σ, 1.2σ, and $< 1\sigma$ (from left to right).

Table 1. Sources with a soft/negative lag detection at $> 2\sigma$ confidence level. (1) Name; (2) XMM-Newton observations; (3) Nominal exposure; (4) Logarithm of the estimated black hole mass, uncertainty, mass estimate technique (R: reverberation mapping, V: stellar velocity dispersion, E: empirical $L_{5100\text{Å}}$ vs R_{BLR} relation), and references ([a] Nelson & Whittle 1995; [b] Oliva et al 1999; [c] Kaspi et al 2000; [d] Vestergaard 2002; [e] Bian & Zhao 2003; [f, g] Peterson et al 2004, 2005; [h] Zhang & Wang 2006; [i] Wang & Zhang 2007; [l] Bentz et al 2009; [m] Zhou et al 2010; [n] Denney et al 2010); (5) Soft and hard X-ray energy bands used for the lag computation; (6) soft/negative lag significance.

Name (1)	Obs ID (2)	Exposure (ks) (3)	Log ($M_{\rm BH}$) (4)	$\Delta E_{\rm soft/hard}$ (keV) (5)	σ (6)
NGC 4395	0142830101	113	5.56±0.14 R, g	0.3-1/1-5	2.8
NGC 4051	0157560101	52	6.24±0.14 R, n	0.3-1/2-5	3.2
	0109141401	122			
	0606320101	46			
	0606320201	46			
	0606320301	46			
	0606320401	45			
	0606321301	33			
	0606321401	42			
	0606321501	42			
	0606321601	42			
	0606321701	45			
	0606321801	44			
	0606321901	45			
	0606322001	40			
	0606322101	44			
	0606322201	44			
	0606322301	43			
Mrk 766	0109141301	130	6.25±0.35 R, l	0.3-0.7/1.5-4	2.9
	0304030301	99			
	0304030401	99			
	0304030501	96			
	0304030601	99			
	0304030701	35			
Ark 564	0006810101	34	6.27±0.50 E, h	0.3-1/2-5	2.6
	0006810301	16			
	0206400101	102			
MCG-6-30-15	0111570101	47	6.30±0.40 V/E, b, m	0.3-0.9/1.5-3	3.6
	0111570201	66			
	0029740101	89			
	0029740701	129			
	0029740801	130			
1H 0707-495	0511580101	124	6.31±0.50 E, e	0.3-1/1-4	5.4
	0511580201	124			
	0511580301	123			
	0511580401	122			
RE J1034+396	0506440101	93	6.57±0.27 E, m	0.3-1/1.5-4.1	2.4
	0561580201	70			
	0655310101	52			
	0655310201	54			
NGC 7469	0112170301	25	7.09±0.05 R, f	0.3-1.5/1.5-5	2.3
	0112170101	19			
	0207090201	79			
	0207090101	85			
Mrk 335	0306870101	133	7.15±0.12 R, f	0.3-0.6/3-5	3.1
	0600540501	83			
	0600540601	132			
PG 1211+143	0112610101	56	7.37±0.12 R, c	0.3-1./1.-5.	3.4
	0208020101	60			
	0502050101	65			
	0502050201	51			
NGC 3516	0107460601	124	7.50±0.05 R, n	0.3-1/1-5	3.1
	0107460701	130			
	0401210401	52			
	0401210501	69			
	0401210601	69			
	0401211001	69			
NGC 6860	0552170301	123	7.59±0.50 E, i	0.3-1/1-5	2.9
Mrk 1040	0554990101	91	7.64±0.40 V, a, m	0.3-1/1-4	3.3
NGC 5548	0089960301	96	7.65±0.13 R, n	0.3-0.9/1.5-4.5	3.0
Mrk 841	0070740101	123	7.88±0.10 E, d	0.3-1/1-5	3.8
	0070740301	148			
	0205340201	73			
	0205340401	30			

References: Nelson C., Whittle M., 1995, ApJS, 99, 67; Oliva E., Origlia L., Maiolino R., Moorwood A. F. M., 1999, A&A, 350, 9O; Kaspi S., et al., 2000, ApJ, 533, 631; Vestergaard M., 2002, ApJ, 571, 733; Bian W., & Zhao Y., 2003, MNRAS, 343, 164; Peterson B. M., et al., 2004, ApJ, 613, 682; Peterson B. M., 2005, ApJ, 632, 808; Zhang & Wang, ApJ, 2006, 653, 151; Wang & Zhang, 2007, ApJ, 660, 1092; Bentz et al, 2009, ApJ, 705, 217; Zhou X.-L., Zhang S.-N., Wang D.-X., Zhu L., 2010, ApJ, 710, 16; Denney K. D., et al, 2010, ApJ, 721, 715.

Table 2. Sources with a marginal negative lag detected at $< 2\sigma$ confidence level. (1) Name; (2) XMM-Newton observations; (3) Nominal exposure; (4) Logarithm of the estimated black hole mass, uncertainty, mass estimate technique (R: reverberation mapping, V: stellar velocity dispersion, E: empirical $L_{5100\text{Å}}$ vs R_{BLR} relation), and references ([a] Oliva et al. 1995; [b] Peterson et al 2004; [c] Wang, Watari & Mineshige 2004; [d] Zhang & Wang 2006; [e] Zhou & Wang 2005; [f] Vestergaard & Peterson 2006; [g] Jin et al 2009; [h] Markowitz 2009; [i] Wang, Mao & Wei 2009; [l] Winter et al 2009); (5) Soft and hard X-ray energy bands used for the lag computation; (6) soft/negative lag significance.

Name (1)	Obs ID (2)	Exposure (ks) (3)	Log ($M_{\rm BH}$) (4)	$\Delta E_{\rm soft/hard}$ (keV) (5)	σ (6)
IRAS F12397+3333	0202180201	80	6.66±0.50 E, d	0.3-1/1-5	1.6
IRAS 13224-3809	0110890101	64	6.76±0.50 E, e	0.3-1/1-4	1.9
Mrk 1502	0110890301	22	7.44±0.50 E, f	0.3-1/1-5	1.4
	0300470101	86			
Mrk 279	0083960101	33	7.54±0.12 R, b	0.3-1/1-5	1.2
	0302480401	60			
	0302480501	60			
	0302480601	38			
IRAS 13349+2438	0096010101	65	7.74±0.50 E, c	0.3-0.8/0.8-2	1.8
	0402080201	48			
	0402080301	69			
RX J0136.9-3510	0303340101	54	7.89±0.50 E, g	0.3-1/1-5	1.9
Mrk 509	0130720101	32	8.16±0.04 R, b	0.3-1/1-4	1.9
	0130720201	44			
	0306090201	86			
	0306090301	47			
	0306090401	70			
IC 4329a	0147440101	136	8.34±0.30 V, h	0.3-0.8/1-4	1.2
ESO 198-G24	0067190101	34	8.48±0.50 E, e	0.3-1/1-5	1.8
	0305370101	122			
ESO 511-G030	0502090201	112	8.66±0.50 E, l	0.3-1/1-5	1.1
NGC 4593	0059830101	87	6.73±0.43 R, b	0.3-1/1-5	<1
Mrk 110	0201130501	47	7.40±0.11 R, b	0.3-1/1-5	<1
NGC 3783	0112210101	40	7.47±0.08 R, b	0.3-1/1-5	<1
	0112210201	138			
	0112210501	138			
IRAS 05078+1626	0502090501	62	7.55±0.50 E, i	0.3-1/1-5	<1
MCG -5-23-16	0112830401	25	7.92±0.40 V, a	0.3-1/1-5	<1
	0302850201	132			
Mrk 704	0300240101	22	8.11±0.50 E, i	0.3-1/1-5	<1
	0502091601	98			
PDS 456	0041160101	47	8.91±0.50 E, e	0.3-1/1-5	<1
	0501580101	92			
	0501580201	90			

References: Oliva E., Origlia L., Kotilainen J. K., Moorwood A. F. M., 1995, A&A, 301, 55; Peterson B. M., et al., 2004, ApJ, 613, 682; Wang J.-M., Watari K.-Y., & Mineshige S., 2004, ApJ, 607, 107; Zhang & Wang, ApJ, 2006, 653, 151; Zhou X.-L., & Wang J.-M., 2005, ApJ, 618, 83; Vestergaard M., & Peterson B. M., 2006, ApJ, 641, 689; Jin C., Done C., Ward M., Gierliński M., Mullaney J., 2009, MNRAS, 398, 16; Markowitz A., 2009, ApJ, 698, 1740; Wang J., Mao Y. F., & Wei J. Y., 2009, AJ, 137, 3388; Winter L. M., Mushotzky R. F., Reynolds C. S., Tueller J., 2009, ApJ, 690, 1322